

Oxygen scavenging by lithium zincates: the synthesis, structural characterisation and derivatisation of $[\text{Ph}(2\text{-C}_5\text{H}_4\text{N})\text{N}]_2\text{ZnRLi}\cdot n\text{thf}$ ($\text{R} = \text{Bu}^t, \text{Bu}^n; n = 1, 2$)

Sally R. Boss, Robert Haigh, David J. Linton and Andrew E. H. Wheatley*

Department of Chemistry, University of Cambridge, Lensfield Road, Cambridge, UK CB2 1EW

Received 8th April 2002, Accepted 19th June 2002

First published as an Advance Article on the web 25th July 2002

The 1 : 2 reaction of ZnMe_2 with *N*-2-pyridylaniline, $\text{Ph}(2\text{-C}_5\text{H}_4\text{N})\text{NH}$ **1**, affords $[\text{Ph}(2\text{-C}_5\text{H}_4\text{N})\text{N}]_2\text{Zn}$ **10**, the treatment of which with BuLi and *thf* affords the diastereomeric lithium zincate $[\text{Ph}(2\text{-C}_5\text{H}_4\text{N})\text{N}]_2\text{ZnRLi}\cdot n\text{thf}$ ($\text{R} = \text{Bu}^n, n = 2$; **11a**; $\text{R} = \text{Bu}^t, n = 1$, **11b**). The sequential treatment of **10** (either *in situ* or after isolation) with organolithium substrates and molecular oxygen has afforded insights into the oxygen-scavenging capacity of mixed Group 1–Group 12 species. Hence, **10** reacts with Bu^nLi , O_2 and *thf* or dimethoxyethane (*dme*) to give $\{[\text{Ph}(2\text{-C}_5\text{H}_4\text{N})\text{N}]_2\text{ZnOBu}^n\text{Li}\cdot n\text{L}\}_2$ ($n = 1, \text{L} = \text{thf}$, **12a**; $n = 0.5, \text{L} = \text{dme}$, **12b**), with the structural relationship between **11a** and **12a** strongly suggesting that for $\text{R} = \text{Bu}^n$ oxygenation proceeds by insertion into the $\text{Zn}-\text{C}$ bond of an $\{[\text{Ph}(2\text{-C}_5\text{H}_4\text{N})\text{N}]_2\text{ZnR}\}^-$ ion. The employment of Bu^tLi , O_2 and *thf* together with **10** affords only the previously reported complex $[\text{Ph}(2\text{-C}_5\text{H}_4\text{N})\text{N}]_2\text{Zn}[(\mu_3\text{-O})\text{Bu}^t]_2(\text{Li}\cdot\text{thf})_2$ **4**, the formation of which may be rationalised in terms of the Bu^t van der Waals radius and cone angle.

Mixed Li–Zn systems have been used to achieve a wide variety of important chemical transformations. Conjugate addition to enones,¹ the formation of α, β -disubstituted propargylic species and allenes,² halogen–zinc exchange³ and metal carbenoid synthesis⁴ have been effected, and lately dilithium tetraorganozincates have also found applications.⁵ However, the structural chemistry of lithium organozincates is incompletely understood.⁶ While Lewis bases may stabilise ion-separated triorganozincate complexes,⁷ the presence of electron-rich heteroatoms in the zinc-bonded organic residues favours ion-association. In this context $\text{Li}(\mu\text{-C})_n\text{Zn}$ ($n = 1, 2$) motifs dominate the structures of known ion-bonded lithium zincates. Hence, $[\text{2}-(\text{NMe}_2\text{CH}_2)\text{C}_6\text{H}_4]_3\text{ZnLi}\cdot\text{thf}$ reveals a mono-aryl inter-metal bridge⁸ while double bridging is common for tetraorganozincate complexes.^{8,9} Heteroatom bridges have also been reported, with, for example, $(\text{Me}_3\text{Si})_2\text{N}(\text{Me}_3\text{SiCH}_2)_2\text{-ZnLi}\cdot\text{L}$ ($\text{L} = 1,3,5\text{-trimethyl-1,3,5-triazine}$) incorporating a $\text{Zn}(\mu\text{-N})\text{Li}$ linkage.¹⁰

Lewis base centres may be introduced into organometallic molecules in a variety of ways. The insertion of oxygen into a metal–carbon interaction is one such route that has been the subject of much recent study.¹¹ Whereas the oxygenation of organometallic compounds has been probed by the synthesis of new mixed s-block metal compounds,¹² advances have also been made in the templated derivatisation of lithium aluminates using O_2 .¹³ Moreover the sequential reaction of 2-pyridylamines $[\text{R}(2\text{-C}_5\text{H}_4\text{N})\text{NH}]$, $\text{R} = \text{Ph}$ **1**, 3,5-xy **2** ($\text{xy} = \text{xylyl}$), 2,6-xy **3** (1 eq.) with ZnMe_2 , Bu^tLi and thereafter with dry air has been reported to yield various heterobimetallic species.¹⁴ For $\text{R} = \text{Ph}$, $[\text{Ph}(2\text{-C}_5\text{H}_4\text{N})\text{N}]_2\text{Zn}[(\mu_3\text{-O})\text{Bu}^t]_2(\text{Li}\cdot\text{thf})_2$ **4** is formed alongside $\{[\text{Ph}(2\text{-C}_5\text{H}_4\text{N})\text{N}]_2\text{ZnOMeLi}\cdot\text{thf}\}_2$ **5** — the $\text{R} = 3,5\text{-xy}$ analogue (**6**) of which has also been reported.¹⁴ However, the complexity with which such oxygen-capture processes operate is demonstrated by the observation that use of the 2,6-xylyl substrate **3** gives the pseudo-cubic dimer $[\text{Me}(\text{Bu}^t\text{O})\text{Zn}(\text{Bu}^t\text{O})\text{Li}\cdot\text{thf}]_2$ **7** instead. More recently, analogous work using $\text{PhN}(\text{H})\text{-C}(\text{Ph})=\text{NPh}$ (*HAm*) **8**¹⁵ has revealed solvent-dependent oxygen sensitivity, with dimeric $(\text{Am}_2\text{ZnOMeLi}\cdot\text{thf})_2$ **9** (*cf.* **5/6**)¹⁴ crystallising from *thf*.¹⁶ While this observation not only suggested

some generality to the formation of dimers such as **5** and **6**, it once more implied the formal insertion of oxygen into the $\text{Zn}-\text{C}$ bond of an $\{[\text{R}(2\text{-C}_5\text{H}_4\text{N})\text{N}]_2\text{ZnMe}\}^-$ anion. In order to probe this hypothesis we have synthesised and characterised the precursor lithium zincates $[\text{Ph}(2\text{-C}_5\text{H}_4\text{N})\text{N}]_2\text{ZnRLi}$ ($\text{R} = \text{Bu}^n, \text{Bu}^t$) and tested their reactivity towards oxygen.

Results and discussion

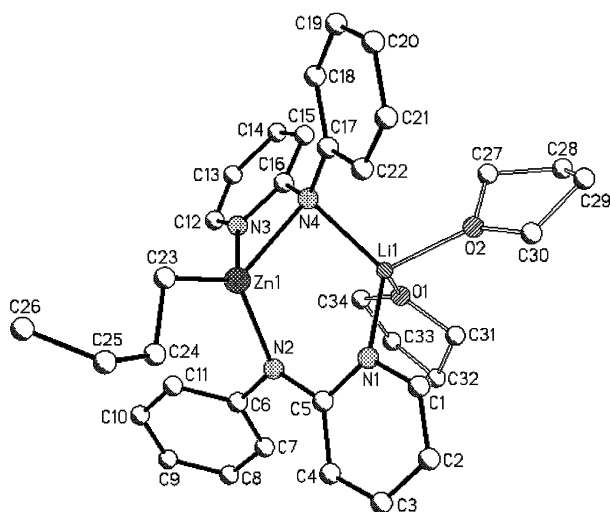
The treatment of ZnMe_2 with 2 eq. *N*-2-pyridylaniline affords an orange solution from which, after heating, a yellow precipitate deposits. Characterisation (see Experimental section) of this material suggests that it is the zinc dianilide $[\text{Ph}(2\text{-C}_5\text{H}_4\text{N})\text{N}]_2\text{Zn}$ **10**. The treatment of this with Bu^nLi affords a single isolable product. ¹H NMR spectroscopy points to the presence of 2-pyridylanilide and Bu^n ligands in a 2 : 1 ratio. The observation of cross peaks in the NOESY between the α -methylene resonance and aromatic signals indicates that in $[\text{C}_6\text{H}_6]$ solution this species is the expected heterobimetallic ate complex. Moreover, NOESY indicates that in hydrocarbon solution this complex is able to adopt a variety of geometries. Nevertheless, one set of resonances is clearly dominant and COSY demonstrates that in this species the signal due to the α -methylene component of the Zn-bonded Bu^n group is at δ 1.75 with the corresponding α -C signal at δ 29.7 by ¹³C NMR spectroscopy. X-Ray crystallography bears out this interpretation, revealing the monomeric bis(*thf*)-solvate $[\text{Ph}(2\text{-C}_5\text{H}_4\text{N})\text{N}]_2\text{ZnBu}^n\text{Li}\cdot 2\text{thf}$ **11a** which crystallises in the space group $P2_1/n$. The alkali metal centre is further supported by the 2-pyridylanilide groups which bridge between each of the two metal centres in the monomer in two distinct ways (Fig. 1). One ligand utilises its formally deprotonated N-centre ($\text{N}4$) to interact with both the Li and Zn centres [$\text{Li}1-\text{N}4$ 2.092(6), $\text{Zn}1-\text{N}4$ 2.135(3) Å; $\text{Li}1-\text{N}4-\text{Zn}1$ 88.62(17)° (Table 1)] while its pyridyl substituent stabilises the Group 12 metal ion [$\text{Zn}1-\text{N}3$ 2.188(3) Å] affording a four-membered ZnN_2C heterocycle. This 2-pyridylanilide ligand thus reveals the same single-centre bridging motif as that shown by the only other reported N-bridged lithium zincate;¹⁰ however the second such

Table 1 Selected bond lengths (Å) and angles (°) for **11a**

Li1–N1	2.054(6)	Zn1–N3	2.188(3)
Li1–N4	2.092(6)	Zn1–N4	2.135(3)
Zn1–N2	2.024(3)	Zn1–C23	1.985(4)
Li1–N4–Zn1	88.62(17)	N2–Zn1–C23	120.36(13)
N1–Li1–N4	110.9(3)	N3–Zn1–C23	127.96(13)
N2–Zn1–N4	113.44(10)	N4–Zn1–C23	119.17(13)
N3–Zn1–N4	62.61(10)		

Table 2 Selected bond lengths (Å) and angles (°) for **11b**

Li1–N1	2.206(6)	Zn1–N3	2.234(3)
Li1–N2	2.032(6)	Zn1–N4	2.116(2)
Li1–N3	2.032(6)	Zn1–C23	1.989(3)
Zn1–N1	2.049(3)		
Li1–N1–Zn1	77.52(17)	N1–Zn1–N4	104.83(10)
Li1–N3–Zn1	77.24(18)	N3–Zn1–N4	62.30(10)
N1–Li1–N2	64.8(2)	N1–Zn1–C23	125.96(12)
N1–Li1–N3	103.2(3)	N3–Zn1–C23	120.75(12)
N2–Li1–N3	110.2(3)	N4–Zn1–C23	123.22(12)
N1–Zn1–N3	101.72(10)		

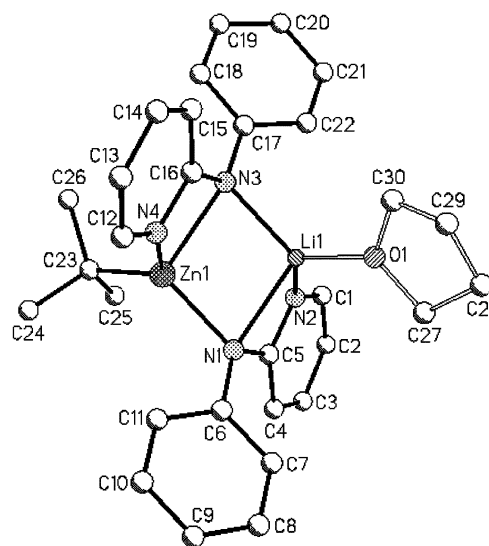
**Fig. 1** Molecular structure of **11a**; hydrogen atoms and Buⁿ disorder omitted.

ligand behaves in a manner akin to that noted recently in $[\text{R}_2\text{ZnOMeLi}\cdot\text{thf}]_2$ ($\text{R} = 2\text{-pyridylanilide},^{14} N,N'\text{-diphenylbenzamidate}^{16}$). Each N-centre within the organic residue bonds to only one metal ion. So whereas (deprotonated) N2 interacts with the Zn^{2+} ion the formally neutral pyridyl N-centre bonds to the alkali metal; the result being that in the solid state the core of **11a** is based on a six-membered ZnN_3CLi metalocycle.

In a similar vein, Bu^nLi combines with **1** to yield a lithium zincate complex, $[\text{Ph}(2\text{-C}_5\text{H}_4\text{N})\text{N}]_2\text{ZnBu}^n\text{Li}\cdot\text{thf}$ **11b**, which reveals a resonance for the Zn–C fragment at δ 33.9 by ^{13}C NMR spectroscopy. Once more, NOESY can be employed to reveal through-space interaction between the Bu^n and aromatic systems, implying retention of the ate complex in $[\text{C}_6\text{H}_6]$ solution. The crystal structure of this compound reveals the reasons for mono(thf)-coordination of the alkali metal centre (Fig. 2). Whereas **11a** revealed amide ligands interacting with Li^+ through only one N-centre each, in **11b** the amide groups form three interactions with the Group 1 ion. One such ligand bridges between the two metals utilising its deprotonated N-centre [Li1–N1 2.206(6), Zn1–N1 2.049(3) Å; Li1–N1–Zn1 77.52(17)° (Table 2)], with further interaction between this residue and the Group 1 metal utilising its pyridyl N-atom [Li1–N2 2.032(6) Å] and affording a four-membered CN_2Li heterocycle. A similar bonding pattern is noted for the second amide ligand [Li1–N3 2.032(6), Zn1–N3 2.234(3) Å; Li1–N3–Zn1 77.24(18)°]

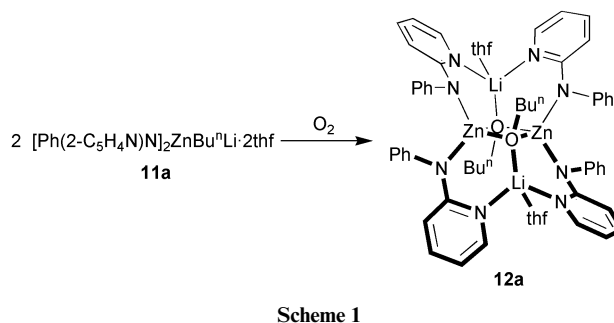
Table 3 Selected bond lengths (Å) and angles (°) for **12a**. Symmetry operations which relate atoms to their $_{-2}$ equivalents: $-x, -y + 1, -z - 1$

Li1–O1	1.916(5)	Zn1–O1	2.0293(16)
Li1–O2	1.968(5)	Zn1–O1_2	2.0239(17)
Li1–N1	2.068(5)	Zn1–N2	1.976(2)
Li1–N3_2	2.077(5)	Zn1–N4	1.969(2)
O1–Zn1–O1_2	86.16(7)	O1–Zn1–N2	117.10(8)
O1–Li1–N1	107.9(2)	O1–Zn1–N4	112.99(9)
O1–Li1–N3_2	108.9(2)	Zn1–O1–Zn1_2	93.84(7)

**Fig. 2** Molecular structure of **11b**; hydrogen atoms omitted for clarity.

notwithstanding that the pyridyl N-centre now supports the zinc [Zn1–N4 2.116(2) Å] and so generates a CN_2Zn ring.

The treatment of a toluene–thf solution of **11a** with O_2 yields only one crystalline product. ^1H NMR spectroscopy reveals retention of the 2 : 1 2-pyridylanilide : Bu^n ratio. However, the Zn-bonded methylene group is no longer observed. Instead, the appearance of a broad signal centred at δ 4.02 and a singlet at δ 64.8 (by ^1H and ^{13}C NMR spectroscopy, respectively) suggests the presence of a ZnOBU^n moiety. Secondly only 1 eq. thf is present in the complex relative to the other organic components. Consistent with these observations, X-ray crystallography reveals this material to be $\{[\text{Ph}(2\text{-C}_5\text{H}_4\text{N})\text{N}]_2\text{ZnOBU}^n\text{Li}\cdot\text{thf}\}_2$ **12a** and, therefore, confirms that a systematic and controllable synthesis of dimeric species of the type previously reported to result from the non-trivial oxygenation of heterobimetallic mixtures^{14,16} is achievable (Scheme 1). Thus,

**Scheme 1**

12a is a C_i -symmetry dimer in the solid state (Fig. 3). However, whereas the previous observation of tetrahedral metal centres in the core (ZnO)₂ ring [mean Zn–O = 2.0266 Å; O–Zn–O = 86.16(7), Zn–O–Zn = 93.84(7)° (Table 3)] in complexes of this type only implied the simple inclusion of oxygen into the Zn–C bond of a lithium triorganozincate anion, a comparison of the structure with that of **11a** clearly establishes that such a process

Table 4 Selected bond lengths (Å) and angles (°) for **12b**. Symmetry operations which relate atoms to their ₂ equivalents: $-x - 1, -y, -z + 1$ and $-x, -y + 1, -z$

Li1–O2	1.929(5)	Zn1–O2	2.0274(18)
Li1–O4	2.096(5)	Zn1–O2_2	2.0410(19)
Li1–N2	2.059(5)	Zn1–N1	1.983(2)
Li1–N4_2	2.055(5)	Zn1–N3	1.987(2)
O2–Zn1–O2_2	87.04(8)	O2–Zn1–N1	112.59(8)
O2–Li1–N2	109.1(2)	O2–Zn1–N3	109.70(8)
O2–Li1–N4_2	105.5(2)	Zn1–O2–Zn1_2	92.96(7)

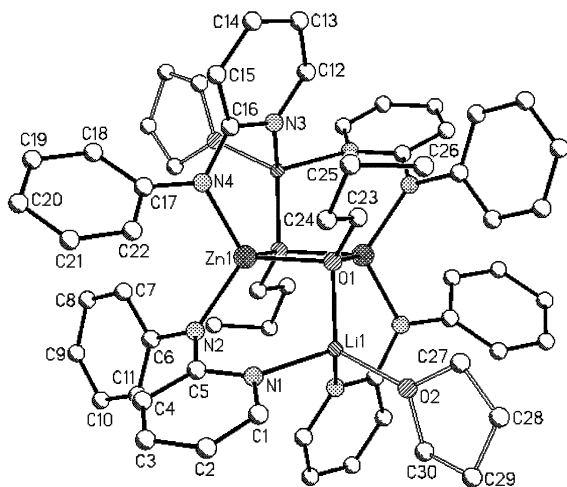


Fig. 3 Molecular structure of dimeric **12a**; hydrogen atoms omitted.

is viable. The Li^+ ions are *anti*-disposed about the core and interact with the O-centres, with dimerisation allowing each metal to also be coordinated by a single pyridyl N-centre in either half of the dimer (mean $\text{Li}-\text{N} = 2.073 \text{ \AA}$). The result is the formation of two LiO -edge-fused pairs of six-membered NCNZNOLi rings where each pair displays one intra-monomer and one inter-monomer $\text{Li}-\text{N}$ interaction. Moreover, the motif noted in the structure of **11a** — whereby a 2-pyridylanilide ligand bridges between lithium and zinc such that each N-centre within the organic residue bonds to only one metal ion — is retained in that of **12a**. Lastly, the dimeric structure of **12a** reveals two types of 2-pyridylanilide ligand with that containing N3/4 being arranged such that its pyridyl component projects *endo* to the $(\text{ZnO})_2$ core whereas that containing N1/2 instead reveals an *exo*-oriented pyridyl ring. In this context, the observation of *double peaks* for each of the aromatic signals in the ^{13}C NMR spectrum of **12a** in hydrocarbon solution is consistent with retention of the solid-state structure.

The stability of the four-membered $(\text{ZnO})_2$ metallocycle in dimers such as **5**, **6**, **9** and — in the present context — **12a** can be demonstrated by the unusual behaviour of dimethoxyethane (dme) in the product (**12b**) obtained by the sequential treatment of **10** with Bu^nLi , dme and O_2 . ^1H NMR spectroscopy suggests a 4 : 2 : 1 2-pyridylanilide : Bu^n : dme ratio and this is borne out crystallographically by the observation that **12b** is $\{[\text{Ph}(2\text{-C}_5\text{H}_4\text{N})\text{N}]_2\text{ZnOBu}^n\text{Li}\cdot 0.5\text{dme}\}_2$. Hence, **12b** reveals the same dimeric configuration and $(\text{ZnO})_2$ core [mean $\text{Zn}-\text{O} = 2.034 \text{ \AA}$; $\text{O}-\text{Zn}-\text{O} = 87.04(8)$, $\text{Zn}-\text{O}-\text{Zn} = 92.96(7)^\circ$ (Table 4)] (Fig. 4) as that noted for its thf-solvated analogue. Rather than adopting its more normal chelating mode,¹⁷ the preference of Li^+ for tetrahedral coordination coupled with the presumed stability of the $(\text{ZnO})_2$ core (and consequently retention of a dimeric structure), causes dme to bridge between metal centres^{17,18} in adjacent aggregates. In consequence, **12b** is rendered polymeric in the solid state.

Whereas in the case of **11a** the direct insertion of an oxygen atom into an existing $\text{Zn}-\text{C}$ bond is observed, the oxygenation of Bu^f complex **11b** gives rise to more complicated behaviour and affords the previously reported¹⁴ trigonal

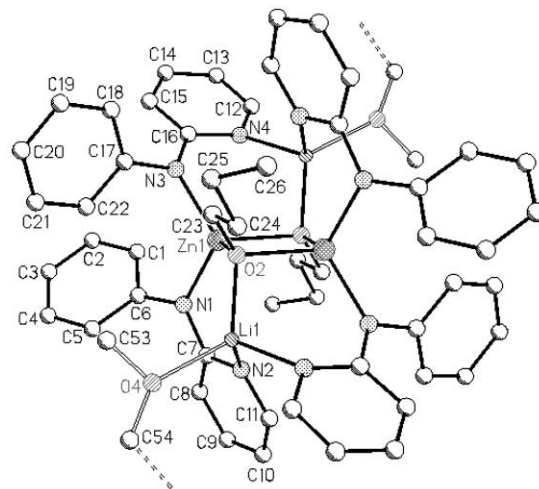


Fig. 4 Molecular structure of polymeric **12b**; hydrogen atoms and minor Bu^n and dme disorder omitted for clarity.

complex $[\text{Ph}(2\text{-C}_5\text{H}_4\text{N})\text{N}]_2\text{Zn}[(\mu_3\text{-O})\text{Bu}^f]_2(\text{Li}\cdot\text{thf})_2$ **4** as the only isolable product in spite of a 1 : 1 $\text{Li} : \text{Zn}$ ratio in the reaction mixture. The synthesis and isolation of **4** from **11b** strongly suggests a steric influence by the R-group on the oxygen scavenging chemistry of the $\{[\text{Ph}(2\text{-C}_5\text{H}_4\text{N})\text{N}]_2\text{ZnR}\}^-$ ($\text{R} = \text{Bu}^n, \text{Bu}^f$) ion. The bridging OBu^n moiety in **12a** is located in an elongated enclosure defined by two pyridyl rings (N1, N3, C1, C16), two Ph groups (C6_2, C7_2, C17, C22) and one thf complexant (O2, C27) (Fig. 5). The dimensions of this cavity can be

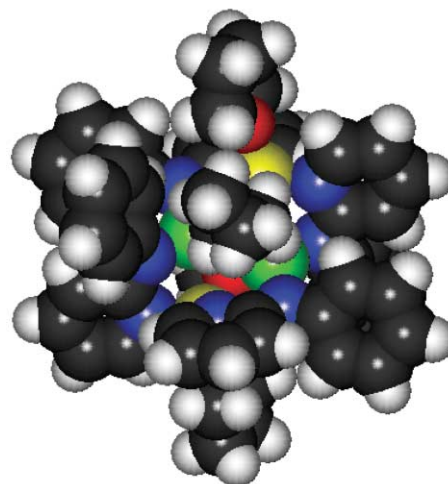


Fig. 5 Space filling diagram of dimeric **12a** showing the incorporation of OBu^n in a pocket defined by three anilide ligands and one thf molecule.

approximated from the non-bonding distances between the van der Waals extrema of these residues, and such an analysis reveals that the topology of the pocket renders it ideal for occupation by OBu^n but *not* by OBu^f . Hence, the observation of $\text{C16} \cdots \text{C27}$ and $\text{N3} \cdots \text{C27}$ non-bonding distances of 7.265 and 7.146 Å, respectively, with $\text{C16} \cdots \text{H27A/B}$ and $\text{N3} \cdots \text{H27A/B}$ distances (calculated on the basis of a riding model — see Experimental section) of 6.794/7.251 Å and 6.792/6.953 Å, respectively. These parameters suggest a gap between van der Waals extrema of between 3.9 Å (for $\text{N3} \cdots \text{H27A}$) and 4.4 Å (for $\text{C16} \cdots \text{H27B}$). Similarly, $\text{N1} \cdots \text{C6}_2$, $\text{N1} \cdots \text{C7}_2$, $\text{C6}_2 \cdots \text{C17}$ and $\text{C6}_2 \cdots \text{C22}$ are 6.833, 6.526, 7.235 and 7.807 Å, respectively (with calculated $\text{N1} \cdots \text{H7}_2$ and $\text{C6}_2 \cdots \text{H22A}$ displacements being 6.044 and 7.358 Å), and these point to distances between van der Waals extrema of 3.3–4.4 Å. The sterically unencumbered n-butyl group exhibits an irregular van der Waals radius

[defined by C23–C24 1.502(4) Å and mean calculated C23–H23, C24–H24 0.990 Å] and a Tolman cone angle¹⁹ of 138.8° and is clearly able to reside in this pocket. However, the more massive 158.0° cone angle¹⁹ and *uniform* 3.1 Å van der Waals radius of the *t*-butyl fragment (mean calculated values for complex **4**) appear to disfavour its inclusion in a cavity of the type revealed by **12a**, thereby suggesting a thermodynamic reason for the formation of **4**. Moreover, a compelling empirical relationship exists between the structure-types represented by these two compounds, with the (2-pyridyl)anilide ligands in **12a** being arranged in a manner that suggests an intimate relationship with the structure of **4**. Formally, this can be described in terms of the rearrangement of two Zn–O interactions and two Li–O bonds (Fig. 6b) in response to the presence of either one

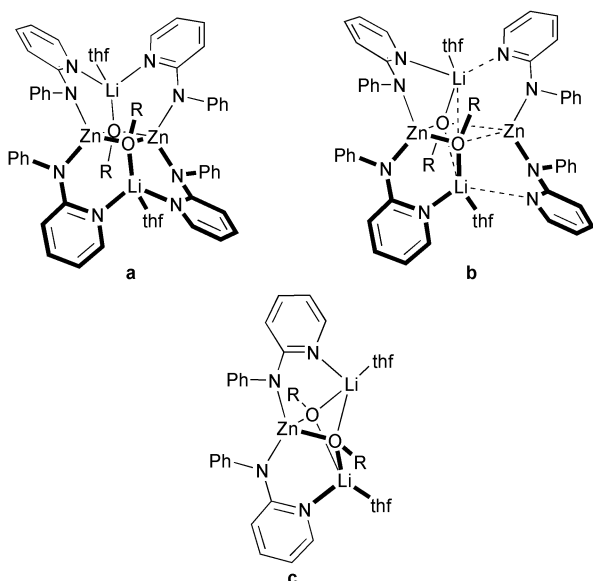


Fig. 6 $\{[\text{Ph}(2\text{-C}_5\text{H}_4\text{N})\text{N}]_2\text{ZnORLi}\cdot\text{thf}\}_2$ (a) can be viewed as incorporating the same components as $[\text{Ph}(2\text{-C}_5\text{H}_4\text{N})\text{N}]_2\text{Zn}[(\mu_3\text{-O})\text{R}]_2(\text{Li}\cdot\text{thf})_2$ (c) upon the formal abstraction (b) of 1 eq. zinc dianilide **10**.

or two molecules of $[\text{Ph}(2\text{-C}_5\text{H}_4\text{N})\text{N}]_2\text{Zn}$ (**10**). The inclusion of two zinc dianilide moieties appears to be concomitant with the formation of a dimer (Fig. 6a) of the type noted for **12a/b** which incorporates the alkoxy moieties within a well defined cavity. However, the coordination of two ROLi fragments by just one molecule of **10** instead yields a trigonal structure (Fig. 6c), akin to that previously seen for complex **4**, in which the steric constraints around the alkoxy groups are considerably diminished.

Conclusions

The treatment of zinc dianilide **10** (*in situ* or after isolation and re-dissolution of the micro-crystalline zinc compound) with a suitable organolithium substrate and then with O_2 has established the viability of (previously postulated)^{14,16} oxygen insertion into the Zn–C bond of a $\{[\text{Ph}(2\text{-C}_5\text{H}_4\text{N})\text{N}]_2\text{ZnR}\}^-$ ion. For sterically undemanding R-groups such as Bu^n this is revealed by the synthesis and characterisation of **11a** and **12a**. That the dimeric motif noted in the latter complex is stable is suggested by the observation that the presence of the potentially Li-chelating agent dme does not result in deaggregation (**12b**).

The presence of a sterically more demanding R-group (Bu^t) in the $\{[\text{Ph}(2\text{-C}_5\text{H}_4\text{N})\text{N}]_2\text{ZnR}\}^-$ precursor to oxygenation leads to a more complicated reaction as evidenced by the isolation of **4**. The intuitively close relationship between the solid-state structures of **12a** and **4** (Fig. 6) is presently being explored through elucidation of the route by which these complexes are generated in solution. Three viable pathways can be suggested: i) zinc dianilide **10** is expelled from an $[\text{Ph}(2\text{-C}_5\text{H}_4\text{N})\text{N}]_2\text{ZnORLi}\cdot n\text{thf}$ monomer, ii) **10** is expelled from an unstable dimer akin to **12a** or, iii) **10** and BuLi are mutually exclusive prior to oxygenation. On the basis of the present data, the first of these options appears most likely, with the structure of **12b** suggesting the stability of a $(\text{ZnO})_2$ ring and both crystallographic and solution NMR data for **11a/b** pointing to the interaction of **10** with a supplied organolithium reagent.

Experimental

Methods and materials

Reactions and manipulations were carried out under an inert atmosphere of dry nitrogen, using double manifold and glove-box techniques. Where appropriate the treatment of air-sensitive reaction mixtures with oxygen was achieved using molecular oxygen (BOC) dried over P_2O_5 (Lancaster). All other chemical reagents were used as received from Aldrich or Lancaster without further purification. Toluene and thf were distilled off sodium or sodium–potassium alloy immediately before use.

NMR data were collected on either a Bruker DPX 400 or DRX 400 (400.12 MHz for ^1H) or a Bruker DRX 500 FT NMR spectrometer (500.05 MHz for ^1H and 125.01 for ^{13}C) at 27 °C or 50 °C. Chemical shifts are internally referenced against deuterated solvents and calculated relative to TMS.

Synthesis and characterisation

[Ph(2-C₅H₄N)N]₂Zn, 10. ZnMe_2 (0.25 ml, 0.5 mmol, 2 M in toluene) was added to *N*-2-pyridylaniline (0.17 g, 1 mmol) in toluene (1 ml). The yellow precipitate which resulted from reflux of this mixture could be isolated or treated with toluene (14 ml) to afford a solution which yielded colourless micro-crystals after 3 d at –30 °C. Both materials analyse as **10**. For the crystalline sample: Yield 140 mg (70%), mp 238–240 °C. Found: C 64.17, H 4.60, N 12.51%. Calc. for $\text{C}_{22}\text{H}_{18}\text{N}_4\text{Zn}$: C 65.44, H 4.49, N 13.87%. ^1H NMR spectroscopy (400 MHz, $[\text{C}_6\text{H}_6]\text{dms}_o$, 27 °C), δ 8.95 (m, br, 1H, Ar), 7.38 (dd, 1H, Ar), 7.24–7.12 (m, 4H, Ar), 6.98–6.51 (m, 0.8H, *PhMe*), 6.84 (d, 1H Ar), 6.76 (m, 1H, Ar), 6.39 (m, br, 1H, Ar), 2.27 (s, 0.5H, *PhMe*).

[Ph(2-C₅H₄N)N]₂ZnBuⁿLi·2thf, 11a. ZnMe_2 (0.25 ml, 0.5 mmol, 2 M in toluene) was added to *N*-2-pyridylaniline (0.17 g, 1 mmol) in toluene (0.75 ml). The mixture was refluxed and then treated with Bu^nLi (0.30 ml, 0.5 mmol, 1.6 M in hexanes) at –78 °C and the resultant suspension was allowed to warm to room temperature. The addition of thf (0.08 ml) afforded a solution which gave **11a** after 2 d at –30 °C. Yield 80 mg (26%), mp 98–100 °C. Found: C 66.44, H 6.84, N 8.50%. Calc. for $\text{C}_{34}\text{H}_{43}\text{LiN}_4\text{O}_2\text{Zn}$: C 66.72, H 7.08, N 9.15%. ^1H NMR spectroscopy (400 MHz, $[\text{C}_6\text{H}_6]\text{dms}_o$, 27 °C), δ 7.94 (m, br, 2H, Ar), 7.43 (m, br, 2H, Ar), 7.36 (dd, 2H, Ar), 7.14 (dd, 2H, Ar), 7.01 (dd, 4H, Ar), 6.83 (m, br, 2H, Ar), 6.19 (m, br, 2H, Ar), 5.99 (m, br, 2H, Ar), 3.48 (m, 8H, thf), 1.75 (m, br, 2H, $\alpha\text{-CH}_2$), 1.49 (m, br, 2H, $\gamma\text{-CH}_2$), 1.34 (m, 8H, thf), 1.04 (t, 3H, CH_3), 0.95 (m, 2H, $\beta\text{-CH}_2$). ^{13}C NMR spectroscopy (125 MHz, $[\text{C}_6\text{H}_6]\text{dms}_o$, 27 °C), δ 167.8, 152.2 (*i*-Ar), 147.3, 138.4, 129.6, 122.7, 120.7, 111.3, 109.7 (*m/p*-Ar), 67.9 (thf), 29.7 ($\alpha\text{-CH}_2$), 25.6 (thf), 25.1 ($\gamma\text{-CH}_2$), 14.3 (CH_3), 13.9 ($\beta\text{-CH}_2$).

[Ph(2-C₅H₄N)N]₂ZnBu^tLi·thf, 11b. ZnMe_2 (0.25 ml, 0.5 mmol, 2 M in toluene) was added to *N*-2-pyridylaniline (0.17 g, 1 mmol) in toluene (1.25 ml). The mixture was refluxed and then treated with Bu^tLi (0.30 ml, 0.5 mmol, 1.7 M in pentane) at –78 °C and the resultant suspension was allowed to attain room temperature. A solution was afforded by the addition of thf (0.08 ml) and after 2 d at –30 °C, **11b** deposited. Yield 146 mg (54%), mp 80–82 °C. Found: C 66.06, H 6.59, N 10.34%. Calc. for $\text{C}_{30}\text{H}_{35}\text{LiN}_4\text{OZn}$: C 66.73, H 6.53, N 10.38%. ^1H

Table 5 Crystallographic data for **11a–12b**

	11a	11b	12a	12b
Formula	C ₃₄ H ₄₃ LiN ₄ O ₂ Zn	C ₃₀ H ₃₅ LiN ₄ OZn	C ₃₀ H ₃₅ LiN ₄ O ₂ Zn	C ₅₆ H ₆₄ Li ₂ N ₈ O ₄ Zn ₂
<i>M</i> _r	612.03	539.93	555.93	1057.77
Crystal system	Monoclinic	Monoclinic	Triclinic	Triclinic
Space group	<i>P</i> 2 ₁ / <i>n</i>	<i>P</i> 2 ₁ / <i>c</i>	<i>P</i> $\bar{1}$	<i>P</i> $\bar{1}$
<i>a</i> /Å	12.3776(7)	9.6358(5)	11.715(2)	11.9618(3)
<i>b</i> /Å	18.8123(6)	17.4699(9)	12.228(2)	12.7891(3)
<i>c</i> /Å	14.0799(8)	16.9408(5)	12.323(2)	19.3890(6)
<i>a</i> °	90	90	107.10(3)	77.647(13)
<i>β</i> °	100.231(2)	93.230(3)	106.27(3)	73.211(15)
<i>γ</i> °	90	90	111.01(3)	74.019(14)
<i>U</i> /Å ³	3226.4(3)	2847.2(2)	1420.3(5)	2700.70(12)
<i>Z</i>	4	4	2	2
<i>ρ</i> _{calc}	1.260	1.260	1.300	0.940
Radiation	Mo-Kα (λ = 0.71069 Å)	Mo-Kα (λ = 0.71069 Å)	Mo-Kα (λ = 0.71069 Å)	Mo-Kα (λ = 0.71069 Å)
<i>μ</i> /mm ⁻¹	0.796	0.891	0.897	1.301
<i>T</i> /K	180(2)	220(2)	180(2)	180(2)
Measured reflections	19551	18191	16302	12229
Unique reflections	5670	4645	6373	9177
<i>R</i> _{int}	0.1123	0.0500	0.0559	0.0536
Final <i>R</i> (<i>F</i>), <i>wR</i> (<i>F</i> ²)	0.0536, 0.1010	0.0597, 0.1309	0.0462, 0.1094	0.0429, 0.1509
Parameters	406	334	343	698
GoF	1.029	1.076	1.056	1.164
Max. peak, hole/e Å ⁻³	±0.504	±0.456	±0.658	±0.996

NMR spectroscopy (500 MHz, [²H₆]C₆H₆, 27 °C), δ 7.84 (m, br, 2H, Ar), 7.45 (m, br, 4H, Ar), 7.38 (m, br, 4H, Ar), 7.02 (m, br, 6H, Ar), 6.22 (dd, br, 2H, Ar), 3.16 (m, 4H, thf), 1.49 (s, 9H, Buⁿ), 1.08 (m, 4H, thf). ¹³C NMR spectroscopy (125 MHz, [²H₆]C₆H₆, 27 °C), δ 167.7, 151.8 (*i*-Ar), 147.2, 138.7, 129.7, 122.3, 120.7, 111.8, 111.1 (*m/p*-Ar), 68.1 (thf), 33.9 (Buⁿ), 25.1 (thf).

[Ph(2-C₅H₄N)N]₂ZnOBuⁿLi·thf]₂, **12a.** As for **11a** in toluene (1 ml) and with the addition of thf (0.4 ml) being followed by the introduction of dry O₂ (*ca.* 15 s), reduction to half-volume and storage at -30 °C for 3 d to give **12a**. Yield 131 mg (49% by ZnMe₂), mp decomp. from 165 °C. Found: C 63.53, H 6.23, N 10.32%. Calc. for C₆₀H₇₀Li₂N₈O₄Zn₂: C 64.81, H 6.35, N 10.08%. ¹H NMR spectroscopy (400 MHz, [²H₆]C₆H₆, 50 °C), δ 8.06 (m, br, 2H, Ar), 7.06–6.97 (m, br, Ar, 6H), 6.86–6.25 (m, 8H, Ar), 6.00 (m, br, 2H, Ar), 4.02 (s, br, 2H, α-CH₂), 3.63 (m, 4H, thf), 1.72 (m, br, 2H, β-CH₂), 1.52 (m, 4H, thf), 1.32 (m, br, 2H, γ-CH₂), 0.94 (m, 3H, CH₃). ¹³C NMR spectroscopy (125 MHz, [²H₆]C₆H₆, 50 °C), δ 168.8, 168.6 (*i*-Ar), 152.0, 151.7 (*i*-Ar), 146.6, 145.5, 137.5, 137.1, 129.2, 129.1, 129.0, 128.9, 124.7, 124.5, 121.2, 120.8, 116.2, 115.9, 110.7, 110.5, 109.8, 109.7 (*m/p*-Ar), 67.6 (thf), 64.8 (α-CH₂), 39.5 (CH₂), 25.6 (thf), 19.5 (CH₂), 14.1 (CH₃).

[Ph(2-C₅H₄N)N]₂ZnOBuⁿLi·0.5dme]₂, **12b.** As for **11a** in toluene (0.8 ml) and with the addition of dimethoxyethane (dme, 0.05 ml) being followed by the introduction of dry O₂ (*ca.* 15 s), storage at -30 °C for 3 d giving **12b**. Yield 100 mg (38% by ZnMe₂), mp 65–67 °C. Found: C 64.86, H 6.12, N 10.31%. Calc. for C₅₆H₆₄Li₂N₈O₄Zn₂: C 63.58, H 6.10, N 10.59%. ¹H NMR spectroscopy (500 MHz, [²H₆]C₆H₆, 27 °C), δ 8.21 (m, br, 2H, Ar), 7.26–7.19 (m, br, 2H, Ar), 7.10–6.69 (m, br, 6H, Ar), 6.54 (m, br, 2H, Ar), 6.39 (m, br, 2H, Ar), 6.27 (m, br, 2H, Ar), 5.96 (m, br, 2H, Ar), 4.07 (s, br, 2H, α-CH₂), 3.35 (s, br, 2H, dme), 3.13 (s, 3H, dme), 1.74 (m, br, 2H, β-CH₂), 1.36 (m, br, 2H, γ-CH₂), 0.98–0.84 (m, br, 3H, CH₃). ¹³C NMR spectroscopy (100 MHz, [²H₆]C₆H₆, 27 °C), δ 168.7, 156.4 (*i*-Ar), 148.5, 137.0, 129.1, 129.0, 122.3, 120.2, 114.6, 109.8, 108.2 (*m/p*-Ar), 72.0 (dme), 62.2 (α-CH₂), 58.4 (dme), 35.1 (CH₂), 19.0 (CH₂), 13.8 (CH₃).

X-Ray crystallography

Data for **11a–12b** were collected using a Nonius Kappa CCD diffractometer equipped with an Oxford Cryostream

low-temperature device (Table 5). Structures were solved by direct methods²⁰ and refined against *F*² using SHELXL-97.²¹ Hydrogen atoms were placed geometrically and allowed to ride during subsequent refinement.

The Buⁿ chain in structure **11a** was found to be disordered while **12b** revealed minor disorder in the Buⁿ and dme residues. In each case, disordered groups were modelled over two orientations, each being refined at half occupancy.

CCDC reference numbers 183652–183655.

See <http://www.rsc.org/suppdata/dt/b2/b203451d/> for crystallographic data in CIF or other electronic format.

Acknowledgements

We thank the UK EPSRC (S. R. B., R. H., D. J. L.) for financial support.

References

- R. A. N. C. Crump, I. Fleming and C. J. Urch, *J. Chem. Soc., Perkin Trans. 1*, 1994, 701.
- P. Knochel, N. Jeong, M. J. Rozema and M. C. P. Yeh, *J. Am. Chem. Soc.*, 1989, **111**, 6474.
- Y. Kondo, M. Fujinami, M. Uchiyama and T. Sakamoto, *J. Chem. Soc., Perkin Trans. 1*, 1997, 799.
- T. Harada, K. Katsuhira, K. Hattori and A. Oku, *J. Org. Chem.*, 1993, **58**, 2958.
- M. Uchiyama, M. Koike, M. Kameda, Y. Kondo and T. Sakamoto, *J. Am. Chem. Soc.*, 1996, **118**, 8733; M. Uchiyama, Y. Kondo, T. Miura and T. Sakamoto, *J. Am. Chem. Soc.*, 1997, **119**, 12372; M. Uchiyama, M. Kameda, O. Mishima, N. Yokoyama, M. Koike, Y. Kondo and T. Sakamoto, *J. Am. Chem. Soc.*, 1998, **120**, 4934.
- D. Linton, P. Schooler and A. E. H. Wheatley, *Coord. Chem. Rev.*, 2001, **223**, 53.
- M. Westerhausen, B. Rademacher and W. Schwarz, *Z. Anorg. Allg. Chem.*, 1993, **619**, 675; M. Westerhausen, B. Rademacher, W. Schwarz and S. Henkel, *J. Naturforsch., Teil B*, 1994, **49**, 199; M. Westerhausen, M. Wieneke, W. Ponikvar, H. Nöth and W. Schwarz, *Organometallics*, 1998, **17**, 1438.
- E. Rijnberg, J. T. B. H. Jastrzebski, J. Boersma, H. Kooijman, N. Veldman, A. L. Spek and G. van Koten, *Organometallics*, 1997, **16**, 2239.
- W. Clegg, P. A. Hunt and B. P. Straughan, *Acta Crystallogr., Sect. C*, 1993, **49**, 2109; H.-O. Fröhlich, B. Kosan, B. Undeutsch and H. Görls, *J. Organomet. Chem.*, 1994, **472**, 1; A. J. Edwards, A. Fallaize, P. R. Raithby, M.-A. Rennie, A. Steiner, K. L. Verhorevoort and D. S. Wright, *J. Chem. Soc., Dalton Trans.*, 1996, 133; R. Wyrwa, H.-O. Fröhlich and H. Görls, *Organometallics*, 1996, **15**, 2833.

- 10 M. Westerhausen, B. Rademacher, W. Schwarz and S. Henkel, *Z. Naturforsch., Teil B*, 1994, **49**, 199.
- 11 A. E. H. Wheatley, *Chem. Soc. Rev.*, 2001, 265.
- 12 G. C. Forbes, A. R. Kennedy, R. E. Mulvey, R. B. Rowlings, W. Clegg, S. T. Liddle and C. C. Wilson, *Chem. Commun.*, 2000, 1759 and refs. cited therein.
- 13 D. R. Armstrong, R. P. Davies, D. J. Linton, P. Schooler, Gregory P. Shields, R. Snaith and A. E. H. Wheatley, *J. Chem. Soc., Dalton Trans.*, 2000, 4304.
- 14 R. P. Davies, D. J. Linton, P. Schooler, R. Snaith and A. E. H. Wheatley, *Chem. Eur. J.*, 2001, **7**, 3696.
- 15 R. P. Davies, D. J. Linton, P. Schooler, R. Snaith and A. E. H. Wheatley, *Eur. J. Inorg. Chem.*, 2001, 619 and refs. cited therein.
- 16 A. D. Bond, D. J. Linton, P. Schooler and A. E. H. Wheatley, *J. Chem. Soc., Dalton Trans.*, 2001, 3173.
- 17 e.g. G. Becker, H.-M. Hartmann, A. Münch and H. Riffel, *Z. Anorg. Allg. Chem.*, 1985, **530**, 29.
- 18 A. Recknagel, F. Knösel, H. Gornitzka, M. Noltemeyer and U. Behrens, *J. Organomet. Chem.*, 1991, **417**, 363; M. A. Nichols and P. G. Williard, *J. Am. Chem. Soc.*, 1993, **115**, 1568; J. Durkin, D. E. Hibbs, P. B. Hitchcock, M. B. Hursthouse, C. Jones, K. M. A. Malik, J. F. Nixon and G. Parry, *J. Chem. Soc., Dalton Trans.*, 1996, 3277; K. W. Henderson, A. E. Dorigo, Q.-Y. Liu and P. G. Williard, *J. Am. Chem. Soc.*, 1997, **119**, 11855.
- 19 T. E. Müller and M. P. Mingos, *Transition Met. Chem.*, 1995, **20**, 533.
- 20 G. M. Sheldrick, *Acta Crystallogr., Sect. A*, 1990, **46**, 467.
- 21 G. M. Sheldrick, SHELXL-97, Program for Crystal Structure Refinement, University of Göttingen, Germany, 1997.